

## 1-Thioangelicin: crystal structure, computer-aided studies and photobiological activity

Daniela Vedaldi <sup>\*</sup>, Alessandro Dolmella, Stefano Moro, Giorgia Miolo, Giampietro Viola, Sergio Caffieri, Francesco Dall'Acqua

*Department of Pharmaceutical Sciences, University of Padua Via F. Marzolo 5, Padua 35131, Italy*

Received 28 March 2003; accepted 5 September 2003

### Abstract

1-Thioangelicin is a furocoumarin analog synthesized to investigate the role of the substitution of sulfur for oxygen in the parent compound angelicin. The compound was examined by X-ray diffraction, and its interaction with DNA, both in the dark and by UVA irradiation, studied by means of linear flow dichroism, chromatography and <sup>1</sup>H NMR. Further insight into the steric and electronic features of 1-thioangelicin has been reached through theoretical calculations, including molecular mechanics optimization, docking studies and frontier molecular orbital investigations. The experimental data indicate that thioangelicin is able to intercalate in the DNA helix and subsequent irradiation yields a *cis*-*syn* adduct, in agreement with theoretical calculations within the lower/higher singly occupied molecular orbital formalism. Antiproliferative activity has been assessed on Balb/c 3T3 cultured cells.

© 2003 Elsevier SAS. All rights reserved.

**Keywords:** Furocoumarins; DNA interactions; X-ray structure; Theoretical calculations

### 1. Introduction

Furocoumarins are a family of natural and synthetic compounds used for the photochemotherapeutic treatment of some skin diseases, lymphomas and other autoimmune disorders [1,2]. Some derivatives of linear furocoumarins (psoralens) have recently been used for sterilizing blood components [3]. Furocoumarins also have pharmacological properties even without irradiation. Some activity against psychological depression has been demonstrated, and they also seem to be useful in the treatment of multiple sclerosis, because of their ability to block potassium channels [4].

The antiproliferative activity of these compounds is mainly connected with the capacity to photoinduce selective lesions to DNA. Although this mechanism is very effective in treating diseases characterized by cell proliferation, such as psoriasis and mycosis fungoides, some side-effects have been observed, including the risk of skin cancer, skin phototoxicity and others. Some angular derivatives, such as angelicins, have good therapeutic activity with fewer side-

effects [5]. Some thio and/or seleno derivatives of psoralen were prepared [6–8] with the aim of obtaining new furocoumarin derivatives. In this regard, we have shown that in the series of thiopsoralens, replacing intracyclic oxygen with sulfur generally leads to increased DNA photobinding [9].

Some new methylthioangelicins have recently been prepared [8] with the aim of studying the effect of substituting oxygen with sulfur in the angular derivatives of psoralen.

In this paper, we studied the sulfur derivative of the parent angular furocoumarin: angelicin, 4*H*-thiopyrano[2,3-*e*]benzofuran-4-one (1-thioangelicin,<sup>1</sup> Fig. 1), to evaluate the role of the intracyclic substitution of oxygen 1 with sulfur. Angelicin was used as reference compound in this study.

The solid-state structure of the title compound was determined by single crystal X-ray diffraction analysis.

Quantum mechanics calculations were carried out to describe the mechanism of the photocycloaddition reaction between 1-thioangelicin and thymine in DNA, its principal photochemical counterpart for the photochemical process.

<sup>\*</sup> Corresponding author.

E-mail address: [daniela.vedaldi@unipd.it](mailto:daniela.vedaldi@unipd.it) (D. Vedaldi).

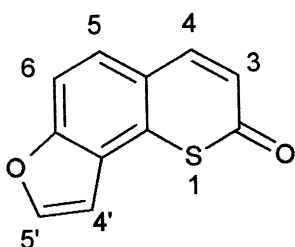


Fig. 1. Molecular structure of 1-thioangelicin.

The dark and photochemical interaction between the compound and DNA has also been studied.

Preliminary experiments on the antiproliferative activity on a cell culture have also been performed.

## 2. Experimental

1-Thioangelicin (*4H*-thiopyrano[2,3-*e*]benzofuran-4-one; 3-oxa-9-thia-cyclopenta[*a*]naphthalen-8-one) was prepared by chemical synthesis by Jakobs et al. [6]. Angelicin, used as reference compound, was donated by Franco Indian Chem. Co., Bombay, India.

### 2.1. X-ray crystallography

A shining, colorless, transparent crystal ( $0.12 \times 0.30 \times 0.05$  mm) was mounted on a glass fiber with epoxy resin. All measurements were made using a Nicolet Siemens R3m/V four-circle diffractometer. Cell constants were obtained from a least-squares refinement, using the setting angles of 30 reflections with  $2\theta > 19^\circ$ .

#### 2.1.1. Crystal data

$C_{11}H_6O_2S$ ,  $M = 202.2$ , orthorhombic,  $a = 12.839(8)$ ,  $b = 3.863(2)$ ,  $c = 17.846(5)$  Å,  $U = 885.1(6)$  Å $^3$ ,  $D_c = 1.518$  g cm $^{-3}$ ,  $Z = 4$ ,  $F(000) = 416$ , space group  $Pna2_1$ , Mo-K $\alpha$  radiation, graphite monochromator,  $\lambda = 0.71073$  Å,  $\mu(\text{Mo-K}\alpha) = 3.3$  cm $^{-1}$ . A total of 817 reflections were collected

Table 2  
Bond lengths (Å)

S(1)–C(2)	1.780(7)
C(2)–O(2)	1.231(9)
C(3)–C(4)	1.340(10)
C(4a)–C(5)	1.412(8)
C(5)–C(6)	1.387(9)
C(6a)–O(7)	1.363(8)
O(7)–C(8)	1.380(8)
C(9)–C(9a)	1.418(9)
S(1)–C(9b)	1.755(6)
C(2)–C(3)	1.404(10)
C(4)–C(4a)	1.451(9)
C(4a)–C(9b)	1.369(8)
C(6)–C(6a)	1.368(9)
C(6a)–C(9a)	1.399(8)
C(8)–C(9)	1.348(11)
C(9a)–C(9b)	1.402(8)

using the  $\omega$ – $2\theta$  scan technique to a maximum  $2\theta$  value of  $50^\circ$ . The structure was solved by direct methods and refined by full-matrix least squares. Anisotropic thermal parameters were only assigned to atoms heavier than carbon in order to reduce the number of variable parameters (given the low reflection power of the crystal there was a paucity of observed reflections). All hydrogen atoms were placed in calculated positions and included in structure factors. The final cycles of refinement were based on 632 observed reflections ( $F_o > 4\sigma(F_o)$ ) and 72 parameters, and converged with  $R = 0.038$  and  $R_w = 0.052$ . No significant electron density was observed in the final difference map, the largest peak being  $0.2$  eÅ $^{-3}$ . Final atomic coordinates and equivalent thermal parameters for the non-hydrogen atoms are given in Table 1, while bond distances and angles are given in Tables 2 and 3, respectively. Structure determination and refinement were performed with the SHELXTL-PLUS program system [10].

#### 2.1.2. Calculations

All work was carried out on a SGI IRIS-4D 320 VGX (IRIX 4.0.5). A series of molecular mechanics (MM, DIS-

Table 1  
Atomic coordinates ( $\times 10^4$ ) and equivalent isotropic displacement coefficients (Å $^2 \times 10^3$ )<sup>a</sup>

	$x$	$y$	$z$	$U_{eq}$
S(1)	686(1)	2698(4)	8047	47(1)
C(2)	1301(6)	3200(18)	8934(4)	56(2)
O(2)	810(4)	2064(16)	9473(3)	83(2)
C(3)	2281(5)	4803(19)	8968(4)	57(2)
C(4)	2838(5)	5968(18)	8386(4)	51(2)
C(4a)	2525(4)	5780(15)	7605(3)	36(1)
C(5)	3200(4)	7101(15)	7050(4)	44(1)
C(6)	2970(5)	6905(17)	6292(4)	47(1)
C(6a)	2031(5)	5426(17)	6119(4)	42(1)
O(7)	1648(3)	4932(12)	5415(3)	57(2)
C(8)	693(5)	3332(19)	5495(5)	62(2)
C(9)	468(5)	2820(17)	6225(4)	51(2)
C(9a)	1319(4)	4133(15)	6643(3)	37(1)
C(9b)	1590(4)	4356(15)	7402(3)	35(1)

<sup>a</sup> Equivalent isotropic  $U$  defined as one third of the trace of the orthogonalized  $U_{ij}$  tensor

Table 3  
Bond angles (°)

C(2)–S(1)–C(9b)	104.5(3)
O(2)–C(2)–C(3)	125.7(7)
C(4)–C(4a)–C(5)	119.0(5)
C(4a)–C(5)–C(6)	122.2(5)
C(6)–C(6a)–C(9a)	125.0(6)
O(7)–C(8)–C(9)	110.9(7)
C(6a)–C(9a)–C(9b)	117.5(5)
S(1)–C(9b)–C(9a)	116.6(4)
S(1)–C(2)–O(2)	115.4(5)
C(2)–C(3)–C(4)	126.4(7)
C(4)–C(4a)–C(9b)	121.2(5)
C(5)–C(6)–C(6a)	115.5(6)
O(7)–C(6a)–C(9a)	109.2(5)
C(8)–C(9)–C(9a)	106.9(6)
C(9)–C(9a)–C(9b)	136.2(6)
C(4a)–C(9b)–C(9a)	119.9(5)
S(1)–C(2)–C(3)	119.0(5)
C(3)–C(4)–C(4a)	125.4(6)
C(5)–C(4a)–C(9b)	119.8(5)
C(6)–C(6a)–O(7)	125.8(6)
C(6a)–O(7)–C(8)	106.7(5)
C(6a)–C(9a)–C(9)	106.3(5)
S(1)–C(9b)–C(4a)	123.5(4)

COVER), semi-empirical (MOPAC [11]) and quasi-ab initio (DMol) calculations were performed on the title compound by means of the INSIGHTII program package [12]. Geometry optimization was performed starting from solid-state data. Calculations were discontinued when the optimization criteria were met. In MM, the calculation was stopped when the maximum absolute derivative (mad [12]) dropped below  $10^{-5}$  kcal mol $^{-1}$  Å $^{-1}$ . The MOPAC RHF-PM3 calculation was halted when the gradient (GNORM [11]) dropped below  $10^{-1}$ , and the DMol when the ETOL and GRTOL [12] criteria were both met, i.e. when the former dropped below  $10^{-5}$  a.u. and the latter below  $10^{-3}$  a.u. Atomic charges were also calculated.

## 2.2. Computational methodologies

Calculations were performed on a Silicon Graphics O2 R10000 workstation. This study involved the use of consensus dinucleotide intercalation geometry d(ApT) initially obtained using NAMOT2 software [13]. The d(ApT) intercalation site was contained in the center of a decanucleotide duplex of sequences d(5'-ATATA-3') $_2$ . Decamers in B-form were built using the “DNA Builder” module of molecular operating environment (MOE) [14]. Decanucleotide was minimized using Amber94 all-atom force field [15], implemented in MOE, until the rms value of truncated Newton method (TN) was  $<0.001$  kcal mol $^{-1}$  Å $^{-1}$ . The dielectric constant was assumed to be distance independent with a magnitude of 4.

The ground state geometry of 1-thioangelicin was fully optimized without geometry constraints using RHF/AM1 semi-empirical calculations [16]. First excited open-shell

singlet state geometries were fully optimized without geometry constraints using UHF/AM1 semi-empirical calculations. Vibrational frequency analysis was used to characterize the minimum stationary points (zero imaginary frequencies), and the Gaussian98 software package [17] for all quantum mechanical calculations.

1-Thioangelicin was docked into the d(ApT) intercalation site using the flexible MOE-Dock methodology [14]. The purpose of MOE-Dock is to seek favorable binding configurations between a small, flexible ligand and a rigid macromolecular target. The search is conducted within a user-specified 3D docking box, using simulated annealing and a MM force field. MOE-Dock performs a user-specified number of independent docking runs and the resulting conformations and their energies are stored in a molecular database file.

The resulting DNA–ligand intercalated complexes were subjected to Amber94 all-atom energy minimization until the rms of the conjugate gradient was  $<0.1$  kcal mol $^{-1}$  Å $^{-1}$ . Charges for the ligands were imported from the Gaussian output files. The interaction energy values were calculated as the energy of the complex minus the energy of the ligand, minus the energy of DNA:  $\Delta E_{\text{inter}} = E_{(\text{complex})} - (E_{(\text{L})} + E_{(\text{rDNA})})$ .

## 2.3. Interaction with DNA in the dark

### 2.3.1. Linear flow dichroism measurements

The linear flow dichroism ( $\text{LD} = A_{\parallel} - A_{\perp}$ ) of thioangelicin ( $1.7 \times 10^{-4}$  M) in the presence of 3.8 mM DNA containing 2 mM NaCl and 1 mM EDTA was measured on a Jasco J 500 circular dichroism spectrometer converted for LD. The measuring device was designed by Wada and Kozawa [18]. A constant shear gradient of 1000 s $^{-1}$  was used to record the LD spectra, and the base line was taken at 0 gradient.

## 2.4. Interaction with DNA upon irradiation

Irradiation for DNA-photobinding experiments was carried out with two Philips HPW 125 lamps emitting mainly at 365 nm with an irradiation intensity of 58.6 W m $^{-2}$ .

### 2.4.1. Characterization of photoadducts

Cycloaddition products were isolated by acid hydrolysis of a DNA sample irradiated in the presence of 1-thioangelicin, followed by TLC separation (pre-coated silica gel plates 60-F<sub>254</sub> from Merck, Darmstadt, Germany, developed with ethyl acetate/ethanol, 90:10) [19]. A Varian Gemini 200 spectrometer was used for NMR measurements.

### 2.4.2. Evaluation of cross links

Cross links formed in DNA were evaluated by measuring the renaturation capacity of cross-linked DNA after heat denaturation [9].

## 2.5. Cell cultures

Balb/c mouse 3T3 fibroblasts were cultivated in DMEM medium (Dulbecco's modified Eagle medium, Sigma Chem.

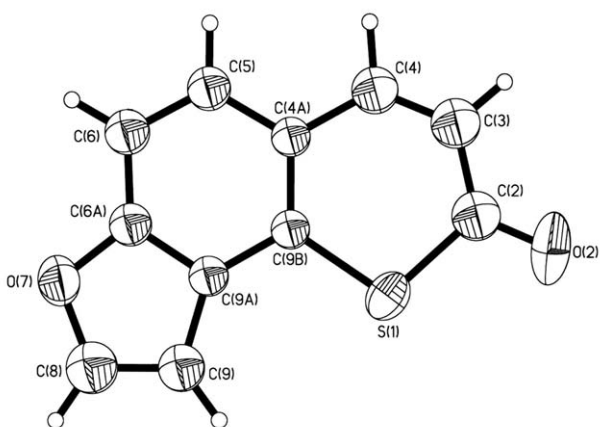


Fig. 2. ORTEP view of the molecule showing the atom numbering scheme and thermal ellipsoids at the 40% probability level. H-atom size has been reduced for clarity.

Co., Milano, Italy) supplemented with 115 units  $\text{ml}^{-1}$  of penicillin G, 115  $\mu\text{g ml}^{-1}$  streptomycin, and 10% fetal calf serum (all from GIBCO Laboratories).

Individual wells of a 96-well tissue culture microtiter plate (IWAKI Japan) were inoculated with 100  $\mu$ l of DMEM containing  $5 \times 10^3$  3T3 cells. The plate was incubated at 37 °C in a humidified 5% incubator for 72 h to form a monolayer of approximately 100% confluence.

After removal of the medium, 100  $\mu$ l of an ethanol solution of the drug, diluted with Hank's balanced salt solution (HBSS, pH = 7.2), was added to each well. The plate was then incubated for 30 min in an atmosphere of 5% CO<sub>2</sub> at 37 °C and then UVA irradiated, the control plate being stored in the dark. After irradiation, the solution was replaced by the medium and the plates were incubated for a further 24 h. Cell viability was assayed by the MTT (3-(4,5-dimethylthiazol-2-yl)-2,5-diphenyltetrazolium bromide) test [20].

### 3. Results

### 3.1. Solid-state structure and computational chemistry evaluation of 1-thioangelicin

### 3.1.1. X-ray crystallography

The structure of thioangelicin, as shown by the ORTEP drawing in Fig. 2, is planar overall, the largest deviations from the mean least-square plane being shown by S(1) (+0.06 Å). The mean displacement of atoms from the mean molecular plane is 0.02 Å, and all dihedral angles show values close to 0 or 180° (the greatest deviations being presented by C(2)–S(1)–C(9b)–C(9a) and C(9b)–S(1)–C(2)–C(3), with 177.2° and 2.5°, respectively). As can be seen in Fig. 3, individual units are stacked one on the top of the other, showing the vertical packing of graphitic layers. The interlayer spacing is 3.863 Å (i.e. *b*-axis), the corresponding value in graphite being 3.35 Å. The solid-state examination does not show short significant intermolecular

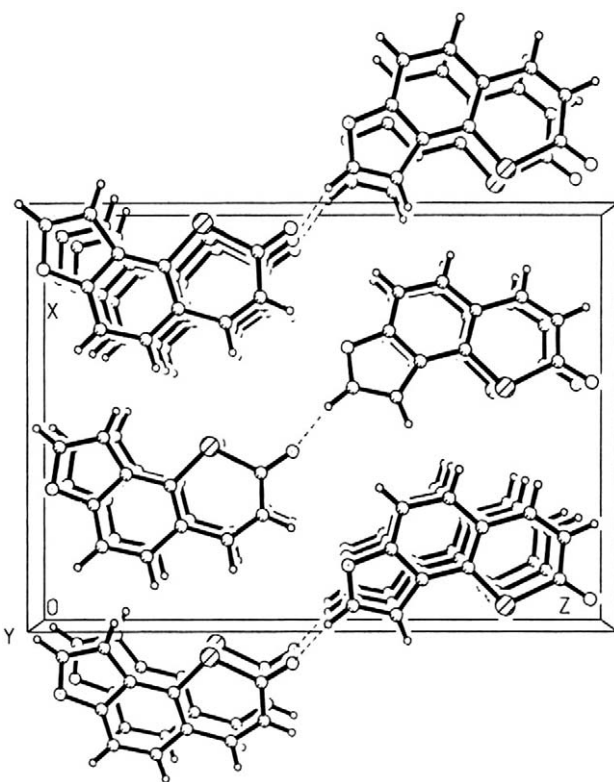


Fig. 3. Packing diagram viewed along the  $b$ -axis showing the only relatively short intermolecular contact (2.52 Å) between H(8) and O(2) at  $-x$ ,  $-y$ ,  $z - 1/2$ .

interactions, with the exception of that indicated in Fig. 3. As a feature, it must be noted that the  $\pi$  interaction is localized between the C(3) and C(4) atoms, as well as between C(8) and C(9). Bond lengths indicate that these two interactions are pure double bonds (C(3)=C(4): 1.340(10) Å; C(8)=C(9): 1.348(11) Å); in the same way, examination of bond length in the central hexa-atomic ring, with values falling between 1.37 and 1.41 Å, depicts the latter as aromatic. Another feature is the unusual widening of the exocyclic angle C(9)–C(9a)–C(9b), which reaches 136.2°. Screening of the Cambridge Structural Database showed that, to the best of our knowledge, only a single deposited structure has a core similar to that of the title compound, i.e. a thiocoumarin derivative studied by Japanese researchers [21].

However, it was difficult to compare the two structures because in the case reported, two crystallographically independent molecules were present, displaying marked differences in values of corresponding bond lengths and angles. For example, the bond length between the two carbons corresponding to C(3) and C(4) in the title compounds shows values of 1.391 and 1.306 Å, respectively, in the two units, but even more evident is the difference in bond length between the carbons corresponding to C(6) and C(6a): 1.533 and 1.249 Å, respectively, in the two units. The same can be said of the bond between the atoms corresponding to C(6a) and C(9a), with 1.248 and 1.505 Å, respectively. The overall appearance of the reported structure is again planar, but there is not much room for further speculation.

Table 4  
Comparison of experimental vs. calculated selected bond lengths (Å) and angles (°)

Parameter	Experimental	MM	MOPAC	DMol
S(1)–C(2)	1.78	1.78	1.82	1.88
C(2)–C(3)	1.40	1.51	1.47	1.43
C(4)–C(4a)	1.45	1.53	1.45	1.42
C(4a)–C(9b)	1.37	1.41	1.40	1.40
C(6)–C(6a)	1.37	1.42	1.40	1.38
C(8)–C(9)	1.35	1.39	1.37	1.36
C(9)–C(9a)	1.42	1.37	1.45	1.43
C(2)–C(3)–C(4)	126.4	122.4	125.8	127.0
C(5)–C(6)–C(6a)	115.5	119.1	116.1	115.9
C(6)–C(6a)–C(9a)	125.0	120.2	123.1	124.2
C(6)–C(6a)–O(7)	125.8	133.0	126.6	126.5
C(9)–C(9a)–C(9b)	136.2	131.4	134.4	134.2

An attempt was made to obtain further structural information by means of a series of calculations at different levels of complexity (from (MM) to quasi-ab initio). The general appearance of the molecule does not really change during the simulations performed in vacuo; in fact, the planarity of the skeleton is even reinforced by calculations (especially MM). This situation is probably due to the lack of a packing force on the isolated molecule. Owing to the rather incomplete parameterization of sulfur, however, the structural features depending on that atom have values significantly different from those expected, and also lead to a deformation of the six-atom heterocycle. The dimensions of the aromatic central ring, instead, are corrected towards ideal benzenoid values, and the same can be said for the 5-membered ring. Small deviations are found in final parameters when starting the MM calculations with localized- or non-localized double bonds. Instead, semi-empirical and quasi-ab initio calculations leave bond distances and angles almost unchanged, again with the noticeable exception of the S(1)–C(2) distance, which reaches 1.82 Å in MOPAC calculations and an unrealistic 1.88 Å in DMol calculations. Table 4 shows the most significant differences in bond lengths and angles between X-ray and calculated data, and a comparison of the atomic charges, as obtained from quasi-ab initio and semi-empirical methods, is reported in Table 5.

### 3.2. Theoretical investigation of photochemical behavior of 1-thioangelicin

Photoreactivity of coumarins and angular furocoumarin derivatives with DNA structure is generally described as [2 + 2] photocycloaddition reaction with the pyridine bases. To describe the mechanism of the photocycloaddition reaction, AM1 semi-empirical calculations were performed to obtain minimum energy geometries and electronic structures for both 1-thioangelicin and thymine, which was found experimentally to be the principle counterpart for the photochemical process.

In accordance with the frontier molecular orbital (FMO) theory [22], when irradiated with UV light, the psoralen moiety can absorb a quantum of radiation which causes one

electron to be promoted from the highest occupied molecular orbital (HOMO) to the lowest unoccupied molecular orbital (LUMO). This excited state is described as the lowest singlet state of the molecule ( $S_1$ ). Angelicin in its  $S_1$  state can undergo intersystem crossing (ISC) to the lowest triplet state ( $T_1$ ). The identity of the excited state (formulated as the lowest singlet or lower triplet states) has been long debated for psoralen and its derivatives [23]. However, as more evidence has been reported for the latter, we first calculated and compared the excited triplet state properties of 1-thiopsoralen [23]. It is plausible to think that one of the singly occupied molecular orbitals, generally named lower singly occupied molecular orbital LSHOMO and higher singly occupied molecular orbital HSLUMO, interacts with one of the thymine molecular orbitals of proper size and symmetry. In accordance with the Fukui theory [24] the interaction energies between reactive species are proportional to the molecular orbital overlap and in inverse proportion to the energy gap between the corresponding molecular orbitals.

Table 5  
Comparison of MOPAC and DMol calculated atomic charges

	DMol	MOPAC
S(1)	0.10	0.13
C(2)	0.08	0.26
O(2)	-0.23	-0.27
C(3)	-0.07	-0.23
H(3)	0.07	0.13
C(4)	-0.03	0.00
H(4)	0.07	0.10
C(4a)	-0.02	-0.10
C(5)	-0.04	-0.05
H(5)	0.06	0.10
C(6)	-0.06	-0.09
H(6)	0.07	0.12
C(6a)	0.06	0.04
O(7)	-0.08	-0.07
C(8)	0.02	-0.02
H(8)	0.08	0.15
C(9)	-0.08	-0.15
H(9)	0.07	0.15
C(9a)	-0.04	-0.08
C(9b)	-0.03	-0.10

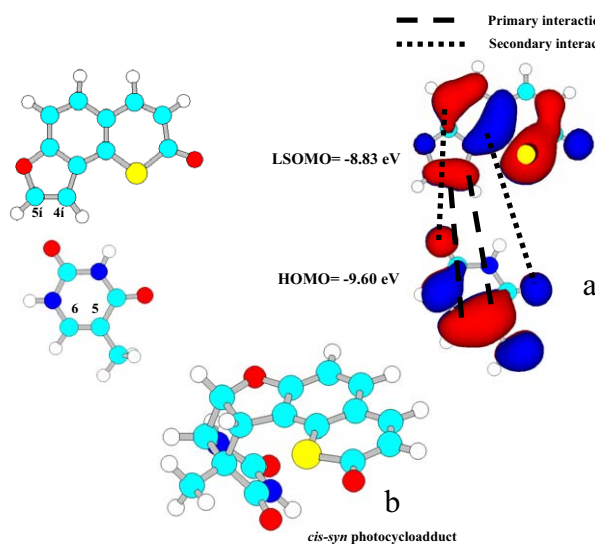


Fig. 4. LSOMO–HOMO combination for the photoreaction of 1-thioangelicin with thymine. Orbital energies are in eV.

As reported in Fig. 4a, AM1 calculations show that there is an energetically favored interaction between the 1-thioangelicin's LSHOMO ( $E_{\text{LSHOMO}} = -8.83$  eV) and the thymine HOMO ( $E_{\text{HOMO}} = -9.60$  eV). Considering the LSHOMO and HOMO coefficients, this interaction is related to the 5,6 double bond of the pyrimidine base and the 4',5' double bond of the 1-thioangelicin. The regioselectivity of the photocycloaddition can be predicted on the basis of maximum frontier orbital overlap [24]. As shown in Fig. 4b, taking the molecular orbitals interaction into account, preference for the endo product (*cis*-*syn* adduct) can be explained as due to “secondary overlap” between the atomic orbitals of thymine and 1-thioangelicin. No such interactions were possible in the exo interaction mode.

Modeling studies have been previously performed to characterize the intercalative binding of psoralen and angelicin derivatives to DNA. In the present study, we have also analyzed in detail the intercalation properties of 1-thioangelicin to better define the steric and electronic requirements during the intercalation process. Flexible docking experiments were performed to calculate the energy changes and optimal geometries corresponding to the intercalative binding of 1-thioangelicin derivatives to A–T base pair in a double helical structure. In agreement with the binding experiments reported above, only alternating purine–pyrimidine steps were considered.

Comparing the theoretical binding energy obtained after the flexible docking analysis seems to confirm that the intercalative process is energetically favored (see Section 2 for details). The docking results are presented in Fig. 5. The orientation of the intercalated chromophore is quite similar to that proposed for other furocoumarins, as it exhibits a predominant component in the direction parallel to the longest dimension of the base pairs. The intercalation geometry is in agreement with the well-known photoreactivity of psoralen derivatives with DNA structure. In fact, after the intercalation

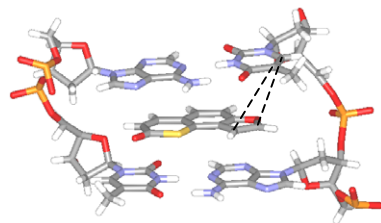


Fig. 5. Stereoview of the energy-minimized model complex between 1-thioangelicin and d(5'-ATATA-3')<sub>2</sub> duplex.

process, the cycloaddition reaction generally occurred between the furan-side or pyrone-side double bond of the furocoumarin moiety and the 5,6 double bond of a thymine ring. This photoreactivity is generally described as a [2 + 2] photocycloaddition reaction with pyrimidine bases.

### 3.2.1. Spectroscopic properties of 1-thioangelicin

The spectrophotometric properties of thioangelicin were studied by comparing an ethanol solution with angelicin (both  $5.2 \times 10^{-5}$  M). A strong red shift of the absorption capacity was observed in comparison with the parent compound. The peculiar absorption peak due to the  $\pi \rightarrow \pi^*$  transition was at 298 nm for angelicin and 322 nm for its sulfur derivative. This property may improve DNA photobinding of the latter, which exhibits an absorption capacity quite distant from the DNA residual absorption capacity. In particular, the absorption coefficient at 365 nm, a wavelength widely used for photobiological experiments, was 55 for angelicin and 243 for 1-thioangelicin.

### 3.3. Interaction with DNA in the dark

Furocoumarins are known to intercalate inside DNA between two base pairs [25]. Evidence of the formation of the complex in the ground state between the thioangelicin and DNA was obtained by spectrophotometric titration experiments, which showed a strong decrease in the molar absorptivity of the compound upon complexation to the macromolecule.

#### 3.3.1. Flow dichroism studies

The capacity of thioangelicin to intercalate into DNA was studied by means of linear dichroism measurements. Using this technique, the long, stiff DNA molecule is oriented in flow, resulting in a peculiar negative dichroism of the macromolecule, with a minimum at 260 nm. When a small planar ligand undergoes intercalation between two base pairs, it assumes an ordered position similar to that of purines and pyrimidines. Therefore, negative dichroism at the wavelength of the chromophore of the ligand can be seen when its transition moment is polarized in parallel with the planar chromophore, as for DNA bases.

Negative linear dichroism was observed (Fig. 6) in the 290–400 nm range, where  $\pi \rightarrow \pi^*$  transitions, which are polarized in the molecule plane [26], are responsible for the strongest absorption of the compound studied here.

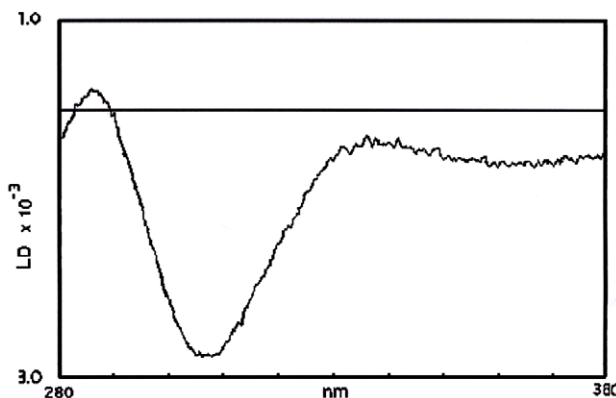


Fig. 6. LD spectrum of the DNA complex formed in the dark by 1-thioangelicin.

#### 3.4. Interaction with DNA upon irradiation

##### 3.4.1. Covalent photoaddition to DNA

DNA irradiated in the presence of thioangelicin acquired a brilliant violet fluorescence ( $\lambda_{\text{exc}} = 350 \text{ nm}$ ,  $\lambda_{\text{em}} = 438$ ), very similar to that shown by furan-side cycloadducts between other furocoumarins and thymine [19].

##### 3.4.2. Isolation of photoadducts

In order to gain evidence of the DNA photobinding of thioangelicin to DNA, it was necessary to isolate and characterize the covalent photoadducts. A solution of DNA was irradiated in the presence of thioangelicin; the excess compound was removed by precipitation of the macromolecule followed by washing with ethanol. DNA was then hydrolyzed at  $100^\circ\text{C}$  in 0.5 N HCl, neutralized and extracted with chloroform. The organic phase was dried and the residue analyzed by TLC. Of the various bands present on the TLC plates, the violet fluorescent one at  $R_f = 0.55$  was scraped, extracted with ethanol and used for NMR measurements (subscript T refers to the thymine moiety):

$^1\text{H}$  NMR (acetone-d6, 200 MHz)  $\delta$ : 1.75 (s, 3H, Me-5<sub>T</sub>), 4.10 (d, 1H, H-4,  $J = 6.4 \text{ Hz}$ ), 4.31 (m, 1H, H-6T), 5.50 (dd, 1H, H-5',  $J = 6.4$  and  $5.4 \text{ Hz}$ ), 6.33 (d, 1H, H-3,  $J = 10.6 \text{ Hz}$ ), 6.85 (broad, 1H, H-1<sub>T</sub>), 6.96 and 7.64 (2 d, 1H each, H-5 and H-6,  $J = 8.5 \text{ Hz}$ ), 7.87 (d, 1H, H-4,  $J = 10.6 \text{ Hz}$ ), 8.7 (broad, 1H, H-3<sub>T</sub>).

These data, in agreement with those of the adducts with thymine isolated from DNA photoreacted with several furocoumarins, allow the adduct to be assigned the *cis-syn* structure shown in Fig. 7.

##### 3.4.3. Cross-link formation

1-Thioangelicin was expected to behave as a monofunctional agent, like most angular furocoumarins, and this property was confirmed. No evidence of cross-link formation was detected after hydroxylapatite column chromatography of DNA irradiated in the presence of the compound.

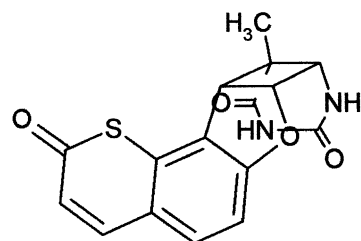


Fig. 7. Molecular structure of the cycloadduct between 1-thioangelicin and thymine formed in DNA.

#### 3.5. Cellular phototoxicity

The phototoxicity of thioangelicin was investigated on a cultured cell line of murine fibroblasts (Balb/c 3T3). Fig. 8 shows the extent of cell survival expressed as a percentage of cell viability, determined with the MTT test after UVA irradiation ( $3.3 \text{ J cm}^{-2}$ ) at different drug concentration. As a comparison, the parent compound angelicin was included in the study. Control experiments with UVA light or drug alone were carried out, and no cytotoxic effects were observed (data not shown).

It can be noted that 1-thioangelicin displayed a significantly higher antiproliferative activity than angelicin. The  $IC_{50}$ , i.e. the drug concentration necessary to induce 50% cell growth inhibition, calculated through linear regression analysis, is  $>30$  and  $11.0 \pm 0.9 \mu\text{M}$  for angelicin and thioangelicin, respectively.

#### Supplementary material

A listing of the crystal data, details of data collection and structure refinement (Table A), anisotropic thermal parameters for S(1), O(2) and O(7) (Table B), hydrogen atom coordinates (Table C) and tables of calculated/observed structure factors (3 pages) are available from the authors upon request.

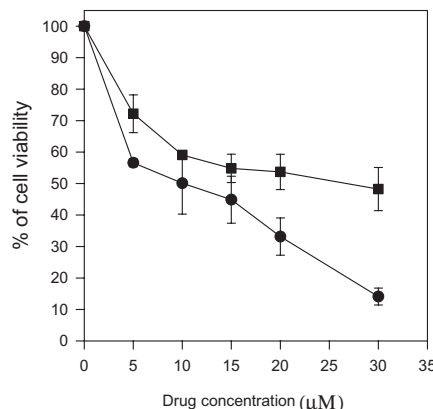


Fig. 8. Percentage of 3T3 fibroblast viability after thioangelicin plus UVA treatment. Cells were treated with the indicated amount of compound and irradiated for 15 min. Viability was measured after 24 h after treatment. ●, thioangelicin; ■, angelicin. Vertical bars indicate standard errors from the mean of three independent experiments.

## Acknowledgements

This research was funded by the Ministero per l'Università e la Ricerca Scientifica e Tecnologica (Rome) and the University of Padova within the Programmi di Ricerca di Interesse Nazionale (Project: Mechanisms of photoinduced processes in homogeneous media and in complex matrices).

## References

- [1] J.A. Parrish, R.S. Stern, M.A. Pathak, T.B. Fitzpatrick, in: G.D. Regan, J.A. Parrish (Eds.), *The Science of Photomedicine*, Plenum Publishing Co, New York, 1982, pp. 595–624.
- [2] F.P. Gasparro (Ed.), *Extracorporeal Photochemotherapy: Clinical Aspects and the Molecular Basis for Efficacy*, CRC Press, Boca Raton, 1994.
- [3] L. Lin, D.N. Cook, G.P. Wiesehahn, R. Alfonso, B. Behrman, G.D. Cimino, et al., Photochemical inactivation of viruses and bacteria in platelet concentrates by use of a novel psoralen and long-wavelength ultraviolet light, *Transfusion* 37 (1997) 423–435.
- [4] H. Wulff, H. Rauer, T. During, C. Hanselmann, K. Ruff, A. Wrisch, et al., Alkoxypsoralens, novel nonpeptide blockers of Shaker-type K<sup>+</sup> channels: synthesis and photoreactivity, *J. Med. Chem* 41 (1998) 4542–4549.
- [5] F. Bordin, F. Dall'Acqua, A. Guiotto, Angelicins, angular analogs of psoralens: chemistry, photochemical, photobiological and photochemotherapeutic properties, *Pharmacol. Ther.* 52 (1991) 331–363.
- [6] A.E. Jakobs, L.E. Christiaens, M.J. Renson, Synthesis of monosulphur and monoselenium analogues of psoralen, *Tetrahedron* 50 (1994) 9315–9324.
- [7] A.E. Jakobs, J. Piette, 1-Thiomethoxsalen and 1-thiopsoralen: synthesis, photobiological properties and site specific reaction of thiopsoralens with DNA, *J. Med. Chem* 38 (1995) 869–874.
- [8] P. Rodighiero, G. Pastorini, A. Chilin, A. Marotto, Synthesis of methyl derivatives of linear and angular thienocoumarins and thiopyranocoumarins, *J. Heterocyclic Chem.* 35 (1998) 847–852.
- [9] D. Vedaldi, S. Caffieri, S. Frank, F. Dall'Acqua, A. Jakobs, J. Piette, Sulphur and selenium analogues of psoralen as novel potential photochemotherapeutic agents, *Farmaco* 50 (1995) 527–536.
- [10] G.M. Sheldrick, *SHELXTL-PLUS, Integrated System for Solving, Refining and Displaying Crystal Structures for Nicolet R3m/V*, University of Göttingen, Germany, 1987.
- [11] J.J.P. Stewart, *J. Computer-Aided Mol. Design* 4 (1990) 1 MOPAC Manual 85th ed. 9, A general Molecular Orbital Package.
- [12] BIOSYM Technologies, Inc. (1992), 9685 Scranton Road, San Diego, CA, 92121–27777.
- [13] [13] NAMOT2 (Nucleic Acid Modeling Tool), Los Alamos National Laboratory, Los Alamos, NM.
- [14] [14] Molecular Operating Environment (MOE 200.02), Chemical Computing Group, Inc, 1255 University St., Suite 1600, Montreal, Quebec, Canada H3B 3X3.
- [15] S.J. Weiner, P.A. Kollman, D.T. Nguyen, D. Case, An all-atom force field for simulation of proteins and nucleic acids, *J. Comput. Chem* 7 (1986) 230–238.
- [16] M.J.S.E. Dewar, G. Zoebisch, E.F. Healy, AM1: a new general purpose quantum mechanical molecular model, *J. Amer. Chem. Soc.* 107 (1985) 3902–3909.
- [17] M. Frisch, G.W. Trucks, H. Schlegel, G. Scuseria, M. Robb, J. Cheeseman, et al., Gaussian 98 (revision A6), Gaussian Inc, Pittsburgh, PA, 1998.
- [18] A. Wada, S. Kozawa, Instrument for the studies of differential flow dichroism of polymer solutions, *J. Polymer Sci.* 42 (1964) 853–864.
- [19] S. Caffieri, P. Rodighiero, D. Vedaldi, F. Dall'Acqua, Methylallopssoralen-thymine 3,4 and 4',5'-monoadducts formed in the photoreaction with DNA, *Photochem. Photobiol* 42 (1985) 361–366.
- [20] G. Viola, G. Miolo, D. Vedaldi, F. Dall'Acqua, In vitro studies of the phototoxic potential of the antidepressant drugs amitriptyline and imipramine, *Il Farmaco* 55 (2000) 211–218.
- [21] H. Nakazumi, Y. Kobara, T. Kitao, Synthesis and insecticidal activity of 4-(aminomethyl)-2*H*-1-benzothiopyran-2-ones (thiocoumarins) and related compounds, *J. Heterocycl. Chem* 29 (1992) 135–139.
- [22] R.B. Woodward, R. Hoffmann, *The Conservation of Orbital Symmetry*, Verlag Chemie/Academic Press, Weinheim, 1970.
- [23] P.-S. Song, M.L. Harter, T.A. Moore, W.C. Herdon, Luminescence spectra and photocycloaddition of the excited coumarins to DNA bases, *Photochem. Photobiol* 14 (1971) 521–532.
- [24] K. Fukui, *Theory of Orientation and Stereoselection*, Springer Verlag, Berlin, 1975.
- [25] F. Dall'Acqua, D. Vedaldi, S. Caffieri, A. Guiotto, P. Rodighiero, F. Baccichetti, et al., New monofunctional reagents for DNA as possible agents for the photochemotherapy of psoriasis: derivatives of 4,5-dimethylangelicin, *J. Med. Chem* 24 (1981) 178–184.
- [26] F. Tjerneld, B. Nordén, B. Ljunggren, Interaction between DNA and 8-methoxypsonalen studied by linear dichroism, *Photochem. Photobiol* 29 (1979) 1115–1118.